RESEARCH ARTICLE

annalen der physik
www.ann-phys.org

Temporary Singularities and Axions: An Analytic Solution that Challenges Charge Conservation

Jonathan Gratus, Paul Kinsler, and Martin W. McCall*

An analytic solution for electromagnetic fields interacting with an axion field that violates global charge conservation is constructed. Despite providing a specific example where "physics breaks down" at a singularity, it nevertheless demonstrates that the physical laws on the surrounding spacetime still impose constraints on what is allowed to happen. The construction is valid for a spacetime containing a temporary singularity and a Maxwellian electrodynamics containing a proposed "topological" axion field. Further, the concepts of transformation optics can be applied to show that our specific mathematical solution has a much wider applicability.

1. Introduction

Singularities play an interesting role in physics, and come in many different varieties, from the mathematically and philosophically challenging[1–4] to the more mundane.[5–7] As the place where "physics breaks down" in a black-hole, we have the sense that anything might happen at a singularity. This begs the question: are there things we might drop into a singularity that have fundamental properties that could be erased absolutely? Crossing the event horizon, for example, can lead to the baryon number of matter falling in to a black-hole not being conserved, even if its mass-energy still persists.[8] Alternatively, the reverse scenario is also intriguing: we may intuitively have a sense that since the laws of physics have broken down, anything might emerge from a singularity (see e.g. [9]). Although perhaps most useful as a plot device for science fiction stories, should we as concerned physicists nevertheless check what conservation laws might no longer hold? But, if so, and given that immediately on leaving the singularity the laws of physics must then be followed, how could such artifacts manifest themselves?

In this article we consider the conservation of electric charge. In standard approaches to electromagnetism this is sacrosanct, whether for local charge conservation (i.e. the differential version), or for global charge conservation (the integral version). Although local charge conservation is experimentally observed, and is assumed here, this does not of itself guarantee global charge conservation, which instead arises via either of two mechanisms. These mechanisms are: from local charge conservation and the assumption that the region of spacetime is topologically trivial, or from the assumption that the excitation fields $\boldsymbol{D}$ and $\boldsymbol{H}$ are real physical fields. In order to break global charge conservation it is necessary that both of these mechanisms no longer apply,[10] that is, we need

> an extension to Maxwell's equations where $\boldsymbol{D}$ and $\boldsymbol{H}$ are not fundamental physical fields, but are merely gauge fields for the charge and current,

and

> a topologically non-trivial spacetime $\mathcal{M}$, such as in this article, where we consider spacetimes with a temporary singularity.

In ref. [11] we showed that a non trivial spacetime can in principle break global charge conservation, but without detailing a specific set of electromagnetic constitutive relations that might support this. In ref. [12] a minimal extension to Maxwell's equations was considered where $\boldsymbol{D}$ and $\boldsymbol{H}$ did not appear, and which provided an additional axionic term to the vacuum Maxwell's equations. Using this axionic term, we now give in this article an explicit construction of an electromagnetic field configuration which can lead to the breaking of global charge conservation.

In particular, the classical Maxwell vacuum is augmented in quantum field theory to account for vacuum polarization for intense fields. For example, the strong magnetic fields associated with magnetars induce non-trivial dielectric properties on vacuum,[13] but longer established alternatives for polarization of the vacuum are (e.g.) the Euler–Heisenberg[14] or the Bopp–Podolski model.[15–17] However, in these, the model corresponds to well defined $\boldsymbol{D}$ and $\boldsymbol{H}$, in-effect also demanding they are measureable, when in fact this is not necessary.[18–24] To avoid this unnecessary assumption, an alternative approach based purely

J. Gratus, P. Kinsler
Department of Physics
Lancaster University
Lancaster LA1 4YB, UK
E-mail: dr.paul.kinsler@physics.org
J. Gratus, P. Kinsler
The Cockcroft Institute
Sci-Tech Daresbury
Daresbury WA4 4AD, UK
P. Kinsler, M. W. McCall
Department of Physics
Imperial College London
London SW7 2AZ, UK

The ORCID identification number(s) for the author(s) of this article can be found under https://doi.org/10.1002/andp.202000565

DOI: 10.1002/andp.202000565

on the physically measurable fields $\boldsymbol{E}$ and $\boldsymbol{B}$ was developed,[12] and this is what we use here.

The extension to Maxwell's equations[12] considered the constitutive properties of a background medium on the basis that there may be an axion field ζ that does not derive from an axion scalar field. In contrast, in this article we posit that such an axion field can exist independently in the vacuum, instead of just being a property of some background medium. We call this axion field a topological axion because it is distinct from a standard axion and because it has more interesting topological properties. In the context of electromagnetism, axions are already an established area of research,[25–29] usually arising in the context of an added coupling between the Maxwell fields and the field of an axion particle. Such coupled Maxwell-axion dynamics allow situations where a background axion field can influence the behavior of electromagnetic fields. In the standard Maxwell theory, a piecewise constant axion field for a medium is detectable at boundaries[30] where the response can be equivalently cast as either a perfect electrical, or perfect magnetic conductor.[31] Axionic responses were apparently observed experimentally[32] via the magneto-electric effect in Cr_2O_3. More recently axionic responses have also been proposed[33] and observed[34] in topological insulators. Observations are, however, still controversial, with claims that evidence of violation of the so-called Post constraint[35] can be explained by an admittance that describes surface states.[36]

In the domain of particle physics, axions have been proposed as candidates for dark matter,[37] but as yet no particle axions have been observed. Given this context, any self-consistent axionic model, such as the one we propose here, remains a valid candidate for exploration.

In this article we give the explicit construction for the simplest non trivial spacetime, namely Minkowski spacetime with a point removed, which provides us with both a singularity and a non-trivial topology. However, since the machinery of transformation optics[38–40] can be applied in a spacetime sense,[41–43] we also show that this apparently heavily restricted solution is also valid in the more general case of a temporary singularity, as depicted in **Figure 1**. This may include cases where a black hole forms and then subsequently evaporates.[8,44]

In Section 2 we summarize the key points of a Maxwellian electrodynamics based on first-order operators[12] that dispenses with $\boldsymbol{D}$ and $\boldsymbol{H}$ and admits the topological axion field. In Section 3 we define a temporary singularity and its future. Next, in Section 4 we describe the key parts of the design of both the electromagnetic and the axionic fields, and then in Section 5 construct the solution in a way that conforms to the theoretical constraints. Following this, in Section 6 we show how a transformation optics style approach allows us to show that our solution is not specific to the simple spacetime manifold in which we construct it, but is also valid for more realistic spacetime metrics, potentially even for the case of a forming then evaporating black-hole. Finally, in Section 7 we conclude.

2. Topological Axions

The topological axions we consider here are allowed by a minimal relaxation of Maxwell's equations where the role of the unmeasurable electromagnetic excitation fields $\boldsymbol{D}$ and $\boldsymbol{H}$ is explicitly demoted to that of mere gauge fields for the current. As discussed

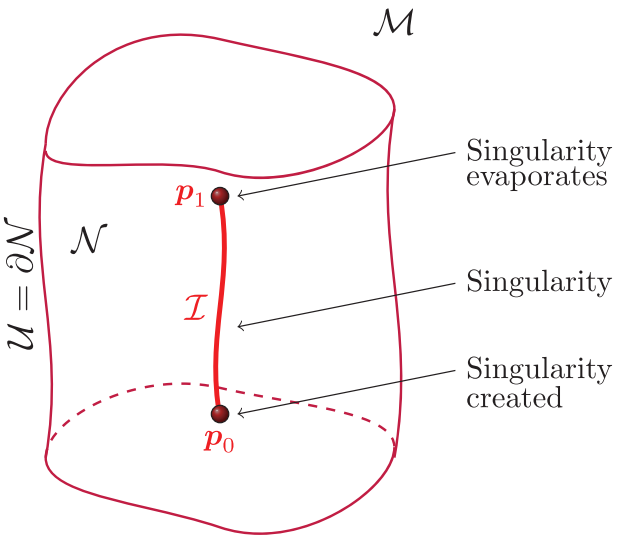

Figure 1. Here we show a temporary singularity. The region of spacetime $\mathcal{N}$ has a boundary $\mathcal{U} = \partial\mathcal{N}$ that encloses a singularity with a finite duration. This might occur, for example, due to the formation at $\boldsymbol{p}_0$ and subsequent evaporation at $\boldsymbol{p}_1$ of a black-hole, which would first create and then remove a metric singularity in spacetime. The temporary singularity $\mathcal{I}$ is not part of $\mathcal{M}$.

in ref. [12], this extension permits a new axionic type of interaction with the electromagnetic field. In addition to dispensing with $\boldsymbol{D}$ and $\boldsymbol{H}$, and in the presence of a spacetime singularity, it has been shown that Maxwell's equations no longer need enforce global charge conservation[11]; but although posing some intriguing possibilities, this proposal did not include any explicit examples of constitutive relations, material configurations, or field distributions.

Here, by attributing this axonic interaction to the presence of a particle-like axion field, we find more general Maxwell's equations for vacuum. Having freed the model from an explicit reference to a material response as implied in ref. [12], we find that there is now scope for an explicit solution that breaks global charge-conservation. The starting point[12] can be briefly summarized as follows. Re-write Maxwell's equations as

$$dF = 0 \qquad \text{and} \qquad \Psi\langle F\rangle = J \tag{1}$$

where[45] $F \in \Gamma\Lambda^2\mathcal{M}$ is the electromagnetic 2–form, $J \in \Gamma\Lambda^3\mathcal{M}$ is the current 3–form, and $\Psi : \Gamma\Lambda^2\mathcal{M} \to \Gamma\Lambda^3\mathcal{M}$ is a non-tensorial "first order operator" that satisfies

$$\begin{aligned} &\Psi\langle\alpha_1 + \alpha_2\rangle = \Psi\langle\alpha_1\rangle + \Psi\langle\alpha_2\rangle, \quad \Psi\langle\lambda\,\alpha\rangle = \lambda\Psi\langle\alpha\rangle, \\ &\text{and} \quad \Psi\left\langle f^2\,\alpha\right\rangle - 2f\,\Psi\langle f\,\alpha\rangle + f^2\,\Psi\langle\alpha\rangle = 0 \end{aligned} \tag{2}$$

for all $\alpha, \alpha_1, \alpha_2 \in \Gamma\Lambda^2\mathcal{M}$, $f \in \Gamma\Lambda^0\mathcal{M}$, and constants $\lambda \in \mathbb{R}$. The angle brackets $\langle\ldots\rangle$ enclosing the arguments to Ψ are used to emphasize its non tensorial nature: notably we have that $\Psi\langle f\alpha\rangle \neq f\Psi\langle\alpha\rangle$. This formulation permits a range of new possibilities,[46] but here we focus on the simplest "axionic" scheme. This means we replace the rather general Equation (1) with an expression

with a more familiar appearance, namely

$$dF = 0 \qquad \text{and} \qquad d \star (\kappa(F)) + \zeta_{\text{top}} \wedge F = J \tag{3}$$

Here κ is the usual constitutive tensor for a medium, and ζ_{top} is a 1–form field generating an additional axion-like interaction. By setting $\Psi\langle F\rangle = d \star (\kappa(F)) + \zeta_{\text{top}} \wedge F$ we see that Equation (3) is an example of Equation (2) since

$$\begin{aligned}
&\Psi\left\langle f^2 F\right\rangle - 2f\,\Psi\langle f\,F\rangle + f^2\,\Psi\langle F\rangle \\
&\quad = d \star (\kappa(f^2\,F)) + \zeta_{\text{top}} \wedge (f^2\,F) - 2f\,d \star (\kappa(f\,F)) \\
&\quad - 2f\,\zeta_{\text{top}} \wedge (f\,F) + f^2\,d \star (\kappa(F)) + f^2\,\zeta_{\text{top}} \wedge F \\
&\quad = d\big(f^2 \star (\kappa(F))\big) - 2f\,d\big(f \star (\kappa(F))\big) + f^2\,d \star (\kappa(F)) \\
&\quad = 2f\,df \wedge \star(\kappa(F)) + f^2\,d \star (\kappa(F)) - 2f\,df \wedge \star(\kappa(F)) \\
&\quad - 2f^2\,d \star (\kappa(F)) + f^2\,d \star (\kappa(F)) = 0
\end{aligned} \tag{4}$$

In a vacuum (i.e. with a trivial κ), we find that adding this axionic interaction naturally adapts the combined Maxwell–Ampère–Gauss equation ($\Psi\langle F\rangle = J$) into

$$\Psi\langle F\rangle = d \star F + \zeta_{\text{top}} \wedge F = J \tag{5}$$

In this formalism, the 2–form F is untwisted, while the ζ_{top} and J are twisted. We emphasize that Equation (5) proposes an extension to the usual vacuum Maxwell equation ($d \star F = J$) in which there is no role (or even sensible definition) for the unmeasurable fields $\boldsymbol{D}$ and $\boldsymbol{H}$.

We denote the axion field ζ_{top} a "topological axion" for two reasons: because it has topological consequences distinct from those axions typically used in models of axion–electromagnetism interaction, and because of the similarities with the standard proposal for the still hypothetical axion particle.

The standard axions are given by a twisted scalar field $\phi_{\text{std}} \in \Gamma\Lambda^0\mathcal{M}$, and their coupling with the electromagnetic field in vacuum defined in the Lagrangian by $\frac{1}{2}\phi_{\text{std}}dA \wedge dA$ in Ref. [27], their Equation (2) is given by their Equations (3) and (4)

$$d \star F + d\phi_{\text{std}} \wedge F = J \tag{6}$$

The similarity between Equations (5) and (6) demonstrates that both interactions are indeed of the same "axionic" type.

We could therefore obtain Equation (5) by insisting that ζ_{std} is exact, that is $d\phi_{\text{std}} = \zeta_{\text{std}}$. However, it is then no longer possible for a field Z_{std} to act as a source for topological axions, since this would imply $Z_{\text{std}} = d\zeta_{\text{std}} = d^2\phi_{\text{std}} = 0$. We show below that to break global charge conservation requires topological axions, for which there is an axion flux Z_{top}, where

$$Z_{\text{top}} = d\zeta_{\text{top}} \neq 0 \tag{7}$$

This is consistent with local charge conservation ($dJ = 0$) provided F and Z_{top} satisfy the constraint $Z_{\text{top}} \wedge F = 0$, as is evident by taking the exterior derivative of Equation (5). The topological axions utilized here are therefore distinct from the standard axion hypothesis, wherein $d\phi_{\text{std}} = \zeta_{\text{std}}$. Nevertheless, since even standard axions have not been detected yet, a widening of axionic theory to include such topological axions is not ruled out by any experimental results to date.

Here we are not directly concerned with the dynamics of ζ_{top} or Z_{top}, but it is nevertheless an interesting consideration. For a massless topological axion, we can define an axion source term $\xi_{\text{top}} \in \Gamma\Lambda^3\mathcal{M}$, and set

$$\xi_{\text{top}} = d \star Z_{\text{top}} \tag{8}$$

so that we could if desired replace Equation (7) with the dynamical equation

$$d \star d\zeta_{\text{top}} = \xi_{\text{top}} \tag{9}$$

In what follows we specify the axion field in terms of the axion flux Z_{top}, but this could be converted into a specification of ξ_{top} using Equation (8) if desired.

Notwithstanding any wider aspects of the field dynamics and the possibility of a Lagrangian (see Appendix C), neither of which are needed for the work herein, we now proceed to consider the primary requirements for our results.

3. The Future Region of a Temporary Singularity

Before discussing how global charge conservation can be violated in a spacetime supporting topological axions, we would like to clarify some aspects of the singularity and its surrounding manifold that together provide the backcloth of our construction.

Specifying whether a spacetime has a temporary singularity is subtle since the singularity itself is not part of the spacetime. There are a plethora of definitions regarding singularities and completeness.[1,3] The approach taken here is to state that a spacetime $\mathcal{M}$ has a temporary singularity if there exists a topological 3–sphere $\mathcal{U} \subset \mathcal{M}$ which is not the boundary of a (compact) 4D ball. We see for example in Figure 1 that $\mathcal{U} = \partial\mathcal{N}$, but $\mathcal{N}$ is not a 4D ball as it has a hole in it. The 3–sphere $\mathcal{U}$ separates $\mathcal{M}$ into two regions which can be called the "inside" and "outside". The inside region is the one that has the temporary singularity, and the outside region goes off to infinity, as depicted on the Penrose diagram[47] in **Figure 2**. In what follows we assume there is precisely one temporary singularity, that is inside the 3–sphere $\mathcal{U}$ there do not exist two or more 3–spheres inside each of which is a temporary singularity, although it is easy to extend the analysis. Also, if we were to consider the case of a temporary black hole, then in addition to containing a temporary singularity, the spacetime would also require the properties of the metric to be specified, that is the existence of an event horizon (see **Figure 3**), and the metric becoming singular as the singularity is approached.

Of course there are many such 3–spheres which surround the temporary singularity and we exploit this to define the future $\mathcal{J}_+$ of the singularity. We say that a point $p \in \mathcal{J}_+$ if for all 3–spheres $\mathcal{U}$ surrounding the singularity and with p outside $\mathcal{U}$ then there exists a causal curve (timelike or lightlike) which passes from $\mathcal{U}$ to p. Conversely, we say that $p \notin \mathcal{J}_+$ if there exists a 3–sphere $\mathcal{U}$ surrounding the singularity, with p on the outside of $\mathcal{U}$, which does not intersect the backward causal cone of p.

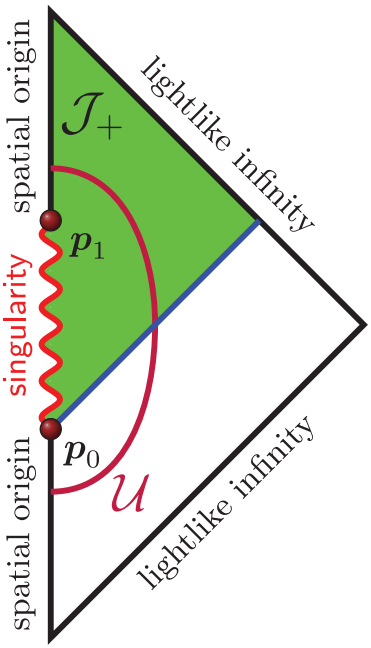

Figure 2. Penrose diagram for a temporary timelike singularity, at the origin, between the points p_0 and p_1. Since light rays travel at 45° on these diagrams, the future of the singularity (its "causal cone") consists of both the light cone or null cone (blue line), and the green region within it. This Penrose diagram contains essentially the same information as the more general view given in Figure 1, but with its lightlike infinity boundaries mapped nonlinearly down to a finite extent. With time passing vertically upward, the radial distance extends horizontally rightward, away from the time axis. The purple line denoted $\mathcal{U}$ is a 3–sphere, and the region inside $\mathcal{U}$ includes the singularity.

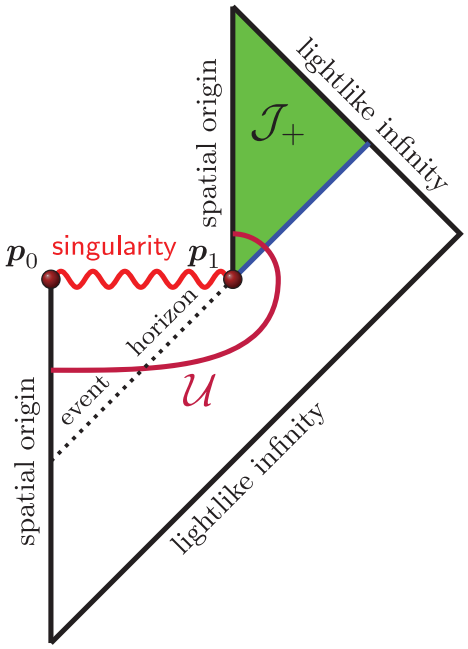

Figure 3. Penrose diagram for a temporary spatial singularity, perhaps due to a forming then evaporating black-hole. Using the same conventions as Figure 2, here the spacelike singularity is instead extended horizontally, thus creating the event horizon, and giving the correct causal structure. The purple line is a 3–sphere $\mathcal{U}$, and the region inside $\mathcal{U}$ includes the singularity.

As an example, let $\mathcal{M} = \mathbb{R}^4\backslash\{0\}$ be Minkowski space excluding the origin, then

$$\mathcal{J}_+ = \left\{ (t,x,y,z) \,\middle|\, t \geq \sqrt{x^2+y^2+z^2} \right\} \tag{10}$$

represents the future of the excised origin as shown in **Figure 4**. This example will be used in Section 5 below to construct a combined electromagnetic and axion field configuration which breaks global charge conservation.

A more general example of a temporary singularity can be constructed by considering a spacetime $\mathcal{M}_{\text{sup}}$ and then excluding a compact set $\mathcal{I} \subset \mathcal{M}_{\text{sup}}$, so that $\mathcal{M} = \mathcal{M}_{\text{sup}}\backslash\mathcal{I}$. Any 3–sphere surrounding $\mathcal{I}$ is not the boundary of a compact 4D ball. An example of $\mathcal{I}$ is a finite interval with end points $p_0, p_1 \in \mathcal{I}$ as shown in Figure 1. Let $\mathcal{J}_+^{\text{sup}}(\mathcal{I}) \subset \mathcal{M}_{\text{sup}}$ be the future causal cone of $\mathcal{I}$. Then $\mathcal{J}_+^{\text{sup}}(\mathcal{I})\backslash\mathcal{I} \subset \mathcal{M}$ and

$$\mathcal{J}_+ = \mathcal{J}_+^{\text{sup}}(\mathcal{I})\backslash\mathcal{I} \tag{11}$$

This is shown in Appendix B. Thus the definition of $\mathcal{J}_+$ coincides with the usual definition of the future causal cone for $\mathcal{I}$.

However, even this more general construction is still not the same as that for a temporary black hole. In Section 6 we will link the above examples using the techniques of transformation optics, in order to show that our conclusions based on a point singularity are in fact significantly more general.

4. Technical Ingredients for Global Charge Conservation Violation

We can now state precisely the technical ingredients leading to our solution that manifests non-conservation of global charge. Since we only consider topological axions, from now on we write the axion field ζ_{top} as just ζ. In order to break global charge conservation, we require a spacetime $\mathcal{M}$ with a temporary singularity, with the future causal cone $\mathcal{J}_+$ as described in Section 3, and the model of electromagnetism described in Section 2, with its topological axions, that is

i) An electromagnetic field $F \in \Gamma\Lambda^2\mathcal{M}$ with support only in $\mathcal{J}_+$.
ii) An electric current $J \in \Gamma\Lambda^3\mathcal{M}$ with support only in $\mathcal{J}_+$.
iii) An axion current $\zeta \in \Gamma\Lambda^1\mathcal{M}$ with support only in $\mathcal{J}_+$; and an axion source $Z_{\text{top}} \in \Gamma\Lambda^2\mathcal{M}$, which also has support only in $\mathcal{J}_+$.

The fields F, the electric current J, the axion field ζ, and the axion flux Z_{top} all satisfy the following criteria:

a) The vacuum Maxwell axion relations Equation (5).
b) The monopole free condition

$$dF = 0 \tag{12}$$

c) The local conservation of charge

$$dJ = 0 \tag{13}$$

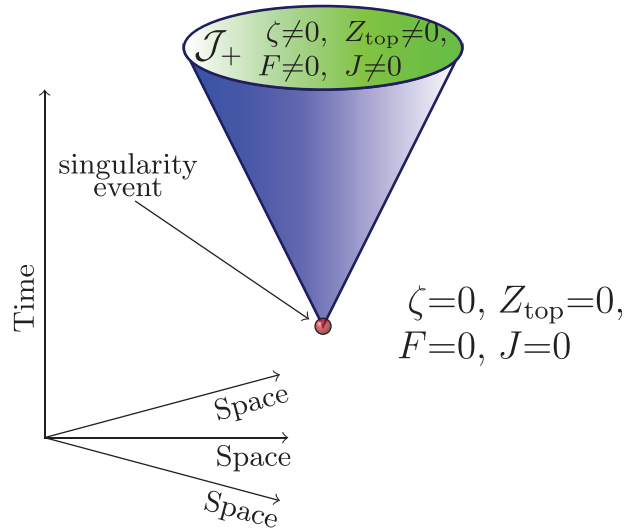

Figure 4. A "singularity event" is excised from spacetime. The causal cone of this singularity is outlined by the light cone (blue) and its interior (green). The resulting non-trivial topology, in concert with the demotion of ***D*** and ***H*** to mere gauge fields, allows global charge conservation to be broken. Our analytic solution achieves this. In the region inside the causal cone the fields vary in time and space. Outside the causal cone they are everywhere zero.

d) The axion field has a source-like flux $Z_{\rm top}$ where

$$d\zeta = Z_{\rm top} \tag{14}$$

The final and most important criterion that we require (i)–(iii) to satisfy is[48]

(e) The total charge is not globally conserved.

Obviously, outside the future causal cone $\mathcal{J}_+$, the current $J = 0$; and for any spatial hypersurface Σ_- which does not intersect the $\mathcal{J}_+$ we have

$$\int_{\Sigma_-} J = 0 \tag{15}$$

Therefore, to show that the last criterion (e) is satisfied we need that for a spatial hypersurface Σ_+ which intersects $\mathcal{J}_+$

$$Q_+ = \int_{\Sigma_+} J \neq 0 \tag{16}$$

"Away from" the temporary singularity, that is if there is a topological 3–sphere which surrounds the temporary singularity, but which does not intersect Σ_+ (the region under consideration), local charge conservation Equation (13) implies global charge conservation. Hence Q_+ is independent of Σ_+ as long as Σ_+ is away from the temporary singularity. Thus for any topological 3–sphere $\mathcal{U}$ surrounding the temporary singularity we deduce (cf. **Figure 5**)

$$Q_+ = \int_{\mathcal{U}} J \tag{17}$$

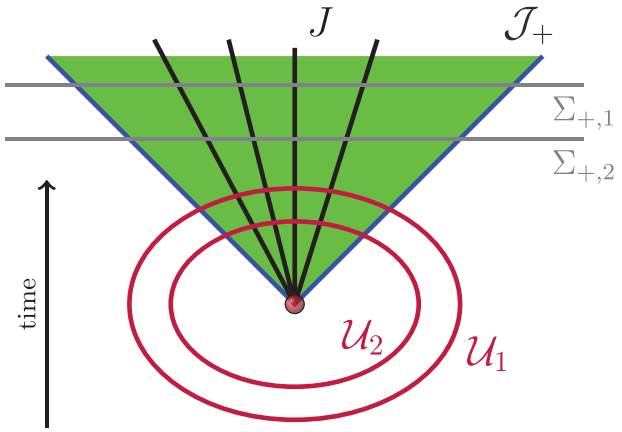

Figure 5. Charge integral, as per Equations (16) and (17); using the representation of forms as lines and surfaces given in Appendix A. The conserved current J can be represented as worldlines (black), and the integral of the form over a hypersurface $\Sigma_{+,i}$ is given by the number of lines that cross it – one may think of it as counting the number of charge at that time. Since there are no charges outside $\mathcal{J}_+$ (bounded by blue lines) then clearly $Q_+ = \int_{\mathcal{U}_1} J = \int_{\mathcal{U}_2} J = \int_{\Sigma_{+,1}} J = \int_{\Sigma_{+,2}} J$.

The axion flux $Z_{\rm top}$ is constrained by the electromagnetic field, and from Equations (5), (12)– (14) we have

$$Z_{\rm top} \wedge F = 0 \tag{18}$$

One way to satisfy this constraint is to have an axion flux entirely separate from the electromagnetic field, that is, for the supports of $Z_{\rm top}$ and F to be disjoint. We might therefore think of $Z_{\rm top}$ as being somewhat analogous to a type-I superconductor that expels magnetic fields. However, this complete separation could be relaxed if we wished to give $Z_{\rm top}$ more freedom.

Notably, if we perform the 3+1 splits of F and $Z_{\rm top}$ with respect to a field of observers $V \in \Gamma T\mathcal{M}$, $g(V, V) = -1$, to give

$$\begin{aligned} F &= E \wedge \widetilde{V} + \star\left(B \wedge \widetilde{V}\right) \\ \text{and} \qquad Z_{\rm top} &= Z_{\rm SE} \wedge \widetilde{V} + \star\left(Z_{\rm SB} \wedge \widetilde{V}\right) \end{aligned} \tag{19}$$

where $\widetilde{V} = g(V, -) \in \Gamma\Lambda^1\mathcal{M}$ is the metric dual of V. Then Equation (18) becomes

$$g(E, Z_{\rm SB}) + g(B, Z_{\rm SE}) = 0 \tag{20}$$

where g is the spacetime metric (see proof in Appendix D). With respect to the observer V the spatial parts of $Z_{\rm top}$ are observed to be $(Z_{\rm SE}, Z_{\rm SB})$, analagous to the way that the spatial parts of F are (E, B). Equation (20) implies that to conserve charge locally we only need a single constraint on the polarizations of $\boldsymbol{E}, \boldsymbol{B}, Z_{\rm SE}, Z_{\rm SB}$. Note that below we will ensure this condition holds for our field solution by specifying the supports of F and $Z_{\rm top}$ to be disjoint. This specification is both convenient and simplifying, although not necessary.

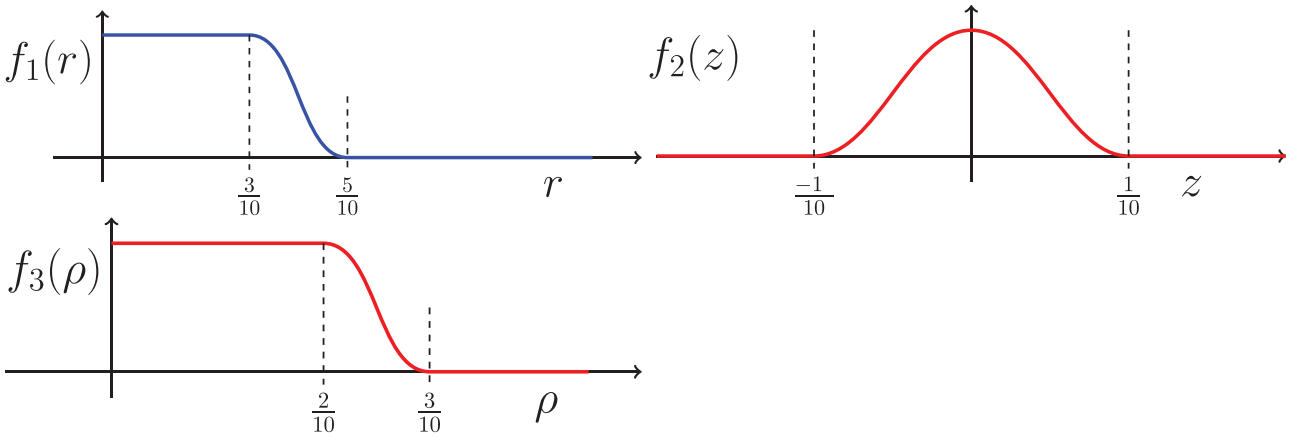

Figure 6. The three smooth "bump functions" used to construct our axisymmetric field solutions. There is one bump function defined for each of the radial r coordinate, the longitudinal z, and the "torus-radial" ρ: that is $f_1(r), f_2(z)$, and $f_3(\rho)$.

5. Construction of ζ and F

We now proceed to define explicit forms for ζ and F that satisfy criteria (a)–(e) above. In what follows, for convenience we specify particular sizes – $\frac{3}{10}$, $\frac{5}{10}$, and so on – but any other convenient sizing that matches the requirements is equally useful.

Note that outside the causal cone $\mathcal{J}_+$, F, and ζ are both zero, and to ensure the solution remains well behaved we construct them using bump functions. For this construction, $\mathcal{M}$ is Minkowski spacetime excluding the origin and $\mathcal{J}_+$ is given by Equation (10). We will use three bump functions, denoted $f_1(r)$, $f_2(z)$, and $f_3(\rho)$. They are smooth, non-negative functions of the type shown in **Figure 6**. Although the functions must have properties that obey specific conditions, they are otherwise arbitrary. The conditions are

$$f_1(r) = \begin{cases} 1 & r < \frac{3}{10} \\ \text{strictly decreasing} & \frac{3}{10} < r < \frac{5}{10} \\ 0 & r > \frac{5}{10} \end{cases} \tag{21}$$

and

$$f_2(z) = \begin{cases} \text{positive for} & |z| < \frac{1}{10} \\ 0 \quad \text{for} & |z| > \frac{1}{10} \end{cases} \tag{22}$$

and

$$f_3(\rho) = \begin{cases} 1 & \rho < \frac{2}{10} \\ \text{strictly decreasing} & \frac{2}{10} < \rho < \frac{3}{10} \\ 0 & \rho > \frac{3}{10} \end{cases} \tag{23}$$

First, note that the above functions can be combined to ensure that the the physical axion field ζ is non-zero only in the regions where required (in cylindrical polars (t, r, θ, z), and with $t > 0$), that is

$$\zeta = f_1\left(\frac{r}{t}\right) f_2\left(\frac{z}{t}\right) d\left(\frac{z}{t}\right) \tag{24}$$

so that

$$Z_{\text{top}} = d\zeta = f_1'\left(\frac{r}{t}\right) f_2\left(\frac{z}{t}\right) d\left(\frac{r}{t}\right) \wedge d\left(\frac{z}{t}\right) \tag{25}$$

where from Equations (21), (22), and (25) the support of Z_{top} is in the region when $|z/t| \leq \frac{1}{10}$ and $\frac{3}{10} \leq r/t \leq \frac{5}{10}$. This arrangement of Z_{top} could be derived from and attributed to its related source ξ_{top}. Note that from Equation (8), the support of ξ_{top} is contained within that of Z_{top}, that is $\text{supp}(\xi_{\text{top}}) \subseteq \text{supp}(Z_{\text{top}})$.

Second, we let the electromagnetic potential A, which will define F, be given by

$$A = f_3\left(\frac{\rho}{t}\right) d\theta \tag{26}$$

where

$$\rho^2 = z^2 + \left(r - \tfrac{4}{10}\right)^2 \tag{27}$$

so that

$$\begin{aligned} F = dA &= f_3'\left(\frac{\rho}{t}\right) d\left(\frac{\rho}{t}\right) \wedge d\theta \\ &= f_3'\left(\frac{\rho}{t}\right) \frac{1}{t^2} (t\, d\rho \wedge d\theta - \rho\, dt \wedge d\theta) \\ &= f_3'\left(\frac{\rho}{t}\right) \frac{1}{t^2 \rho} \left[tz\, dz \wedge d\theta + t\,(r - \tfrac{4}{10}) dr \wedge d\theta - \rho^2 dt \wedge d\theta \right] \end{aligned} \tag{28}$$

From Equation (28) we see that the support of F is when $f_3'(\rho/t) \neq 0$, that is when $\frac{2}{10} \leq \rho/t \leq \frac{3}{10}$.

The specifications in Equations (24) and (26) mean that for $r^2 + z^2 > t^2$, both $F = 0$ and $\zeta = 0$; thus the support of these lie inside the causal cone $\mathcal{J}_+$. Having now defined ζ and F, we can also define J using Equation (5). Further, since the supports of Z_{top} and F are disjoint, Equation (18) is satisfied, which implies, by taking the exterior derivative of Equation (5), that local charge conservation ($dJ = 0$) is preserved.

Thus, by means of this construction of our fields F, ζ, Z_{top}, we have satisfied conditions (a)–(d) as follows: a) from the

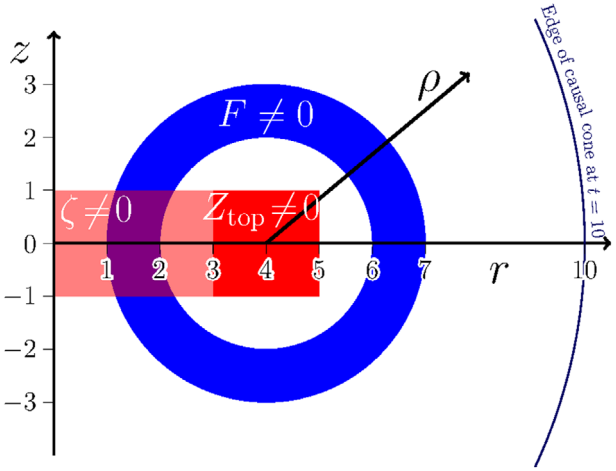

Figure 7. The support of the electromagnetic field F (blue annulus), the axion field ζ (light red and dark red blocks), and the axion flux Z_{top} (dark red block), at the moment when $t = 10$. The region where $\zeta \wedge F \neq 0$ is given by the intersection of the blue and light red regions. The figure is rotated about the z–axis, as seen in Figure 12. This means that the support of F (blue) becomes a solid hollow torus (as in Figures 10 and 11); the support of Z_{top} (dark red) becomes a solid torus with a square cross section (as in Figures 8 and 11); and the support of ζ (light and dark red) becomes a thick disc (as in Figure 9).

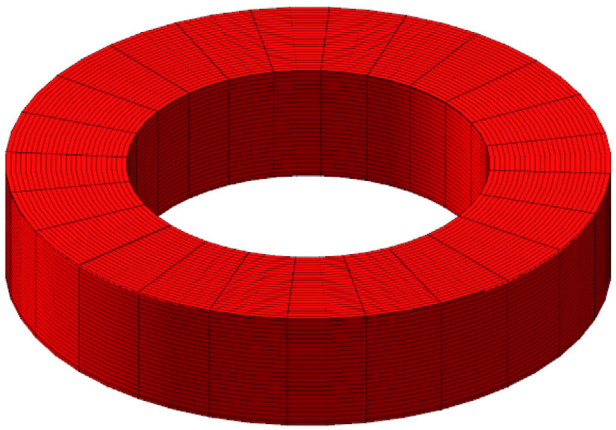

Figure 8. The support of the axion flux Z_{top} (dark red), at $t = 10$, as a 3D plot.

definition of J, b) since $F = dA$, c) from the definition of J in combination with F and ζ being disjoint, and d) from either the definition of Z_{top} itself, or Equation (25). The last condition, e), is demonstrated below in Section 5.2.

The various fields are illustrated in **Figure 7** which delineates the support of each field at $t = 10$, as well in the 3D versions of **Figures 8–11**. A cut at time $t = 10$ and $z = 0$ is shown in **Figure 12**. It is also possible to represent the forms F, Z_{top}, ζ, $\zeta \wedge F$ as dots, lines and surfaces,[49] as described in the Appendix and shown in Figure A1.

5.1. Visualisation

To visualize this electromagnetic construction, it is helpful to consider the different support regions at a single moment in time t.

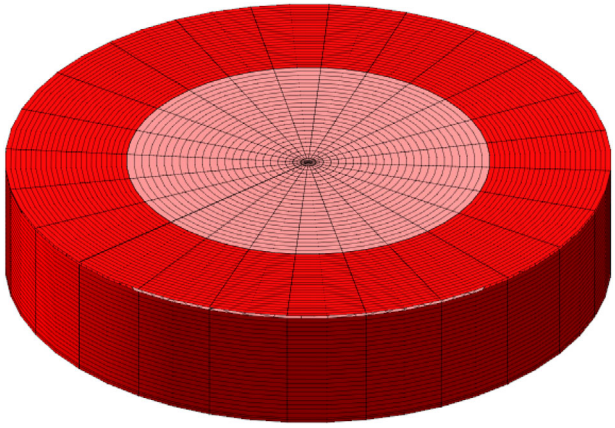

Figure 9. The support of the axion field ζ (both light red and dark red parts) and the axion flux Z_{top} (dark red only), at $t = 10$, as a 3D plot.

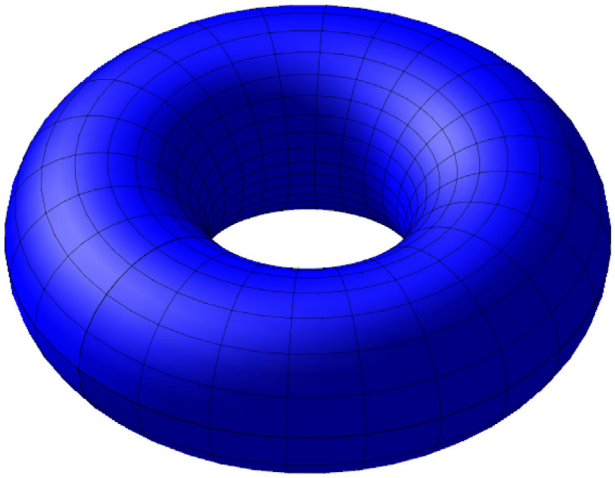

Figure 10. The support of the electromagnetic field F (blue), at $t = 10$, as a 3D plot. According to its definition in Equation (28), and as can be seen from Figure 11, this is not solid, but is a torus-shaped thick but hollow shell.

Following the conventions in Figure 7, they form the following shapes:

1) The region where the axion flux $Z_{\text{top}} \neq 0$ forms a solid torus with a square cross section, as shown in dark red in Figures 8 and 11.
2) The region where the axion field $\zeta \neq 0$ forms a thick disk, which is bounded and includes the region where $Z_{\text{top}} \neq 0$, as shown in Figure 9.
3) The region where the electromagnetic field $F \neq 0$ forms a hollow torus with thick surfaces, as shown in blue on Figures 10 and 11.

5.2. Breaking of Global Charge Conservation: Condition (e)

Since the total charge present before the singularity is exactly zero, any finite amount afterward indicates that global charge conservation has been violated – despite the eminently reasonable starting points (i) to (iii) and criteria (a) to (d).

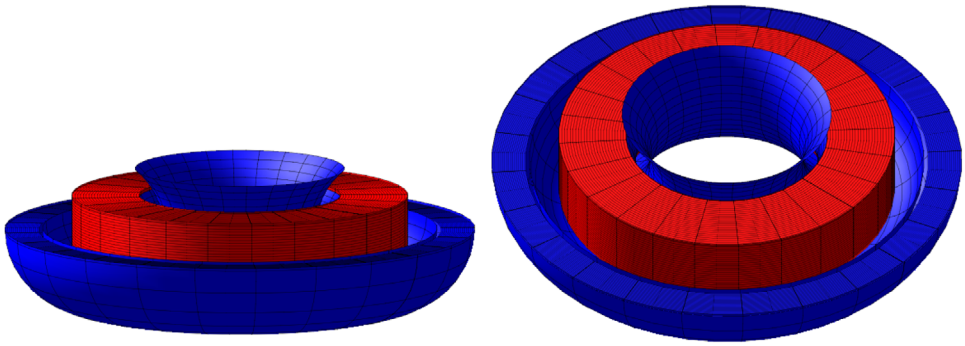

Figure 11. The combined support of the axion flux Z_{top} (red) and a cut of the support of the electromagnetic field F (blue), shown in two views.

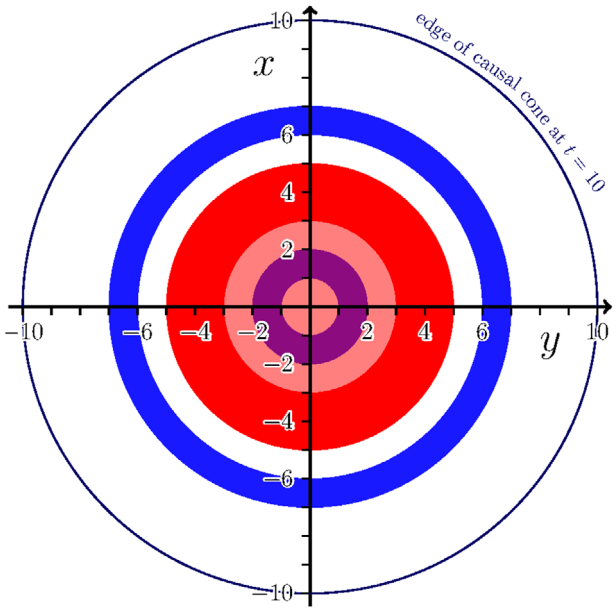

Figure 12. An alternative view of the supports of the electromagnetic field F (blue), the axion field ζ (light and dark red), and the axion flux Z_{top} (dark red), at the moment when $t = 10$ on the slice $z = 0$.

We now explicitly calculate Q_+ the total charge over any time slice after the singularity. This is given by

$$Q_+ = \int_{\mathbb{R}^3} (d \star F + \zeta \wedge F) = Q_{\text{EM}} + Q_{\text{ax}} \tag{29}$$

where $Q_{\text{EM}} = \int_{\mathbb{R}^3} d \star F$ and $Q_{\text{ax}} = \int_{\mathbb{R}^3} \zeta \wedge F$. First, let us consider the contribution Q_{EM}. Such a contribution would appear as a current in the blue region of Figure 7, and the result could easily be calculated. However, we can instead simply observe that for any fixed t time slice, wherein F has compact support, that

$$Q_{\text{EM}} = \int_{\mathbb{R}^3} d \star F = \int_{\text{Boundary}} \star F = 0 \tag{30}$$

This now leaves us to calculate the contribution due to axionic currents, $Q_+ = Q_{\text{ax}} = \int_{\mathbb{R}^3} \zeta \wedge F$. The fact that $\zeta \wedge F$ is closed (i.e. $d\zeta \wedge F = 0$) implies local charge conservation. However, since $\zeta \wedge F$ is not exact (that is, it cannot be written as the exterior derivative of a two-form) the above argument using Stokes' theorem leading to $Q_{\text{EM}} = 0$ does not apply here. In fact, for our constructed ζ and F, we now show that $Q_{\text{ax}} \neq 0$.

Now note that the intersection of the supports of F and ζ is when

$$|z| \leq \tfrac{1}{10} t, \quad r \leq \tfrac{5}{10} t, \quad \left(\tfrac{2}{10} t\right)^2 \leq z^2 + \left(r - \tfrac{4}{10}\right)^2 \leq \left(\tfrac{3}{10} t\right)^2 \tag{31}$$

This implies $r < \frac{3}{10} t$, so that

$$\zeta = f_2\left(\frac{z}{t}\right) d\left(\frac{z}{t}\right) \tag{32}$$

Thus

$$\begin{aligned} \zeta \wedge F &= \frac{1}{t} f_2\left(\frac{z}{t}\right) dz \wedge f_3'\left(\frac{\rho}{t}\right) \frac{1}{t^2 \rho} \quad \times \\ &\qquad \left[tz dz \wedge d\theta + t\left(r - \tfrac{4}{10}\right) dr \wedge d\theta - \rho dt \wedge d\theta\right] \\ &= \frac{1}{t^3 \rho} f_2\left(\frac{z}{t}\right) f_3'\left(\frac{\rho}{t}\right) \quad \times \\ &\qquad \left[t\left(r - \tfrac{4}{10}\right) dz \wedge dr \wedge d\theta - \rho dz \wedge dt \wedge d\theta\right] \end{aligned} \tag{33}$$

Integrating for some specified time $t > 0$ gives the axion contribution to the total charge Q_+:

$$\begin{aligned} Q_+ &= \int_{\theta=0}^{2\pi} \int_{z=\frac{-t}{10}}^{\frac{t}{10}} \int_{r=\frac{t}{10}}^{\frac{3t}{10}} \frac{(r - \frac{4}{10})}{t^2 \rho} f_2\left(\frac{z}{t}\right) f_3'\left(\frac{\rho}{t}\right) dz \wedge dr \wedge d\theta \\ &= 2\pi \int_{z=-\frac{1}{10}}^{\frac{1}{10}} \int_{r=\frac{1}{10}}^{\frac{3}{10}} \frac{(r - \frac{4}{10})}{\rho} f_2(z) f_3'(\rho)\, dz \wedge dr \\ &= 2\pi \int_{z=-\frac{1}{10}}^{\frac{1}{10}} \int_{r=\frac{1}{10}}^{\frac{3}{10}} \frac{(r - \frac{4}{10})}{\sqrt{z^2 + (r - \frac{4}{10})^2}} f_2(z) \quad \times \\ &\qquad f_3'\left(\sqrt{z^2 + \left(r - \tfrac{4}{10}\right)^2}\right) dz \wedge dr \end{aligned} \tag{34}$$

This is clearly independent of t and so is a conserved quantity for $t > 0$. Now we can see that it is possible for $Q_+ \neq 0$; by inspection

of the integrand we have $r - \frac{4}{10} < 0, f_2(z) > 0$ and $f_3'(\rho) < 0$ hence $Q_+ \neq 0$. The non-zero charge originates from both the effusion of F and ζ from the singularity, and the fact that ζ is not exact.

As a result, our claim, which would normally be extremely contentious, is that total charge is not globally conserved, that is our criterion (e) can be met – at least in the context of the electromagnetic model presented here. Our conclusion is that electromagnetic models do not necessarily enforce charge conservation; and this can be said not merely as an abstract claim,[11] but one grounded in the extant mathematical solution we present here. It remains possible, however, that global charge conservation could be enforced by other physical mechanisms.

5.3. Visualisation in Time

Although we have specified the mathematical construction of our non-conserving solution, it is worthwhile describing in more visual terms what such a construction would look like.

This is, in fact, relatively easy. We have already seen the toroidal structure of the axion fluxes and field patterns required in Figures 8–11, but only at a single instance in time. Turning this into a dynamic picture now requires us only to observe that the arguments of the bump functions used in Equations (24) and (26) all contain the factor r/t. Thus any point notionally fixed on the axion flux distribution must hold r/t constant; as time passes and t increases, r also gets larger. The toroidal construction therefore expands, sized in fixed proportion to the spatial cross-section of the future causal cone of the singularity.

Although we have constructed our solution as if the combined axionic and electromagnetic fields were emerging from the singularity, it is easily recast in a time-reversed form where the construction is instead shrinking and vanishing into the singularity.

In Appendix A, we see how to visualize the fields Z_S, ζ, and F as submanifolds.

6. A Temporary Singularity and Transformation Electromagnetism

We would now like to extend the results of the previous sections, which treated a point-like singularity, to allow for a singularity that lives for a finite time.

Let $\hat{\mathcal{M}}$ with metric $\hat{g}$ be a spacetime which represents a temporary singularity as shown in Figure 1. We assume that a diffeomorphism $\phi : \hat{\mathcal{M}} \to \mathcal{M}$ can be constructed such that

α) Any topological 3–sphere which surrounds the temporary singularity in $\hat{\mathcal{M}}$ is mapped to a topological 3–sphere which surrounds the instantaneous singularity in $\mathcal{M}$; see **Figure 13**.

β) The pre-image $\phi^{-1}(\mathcal{J}_+)$ of the forward causal cone of the origin in $\mathcal{M}$ is enclosed within the forward causal cone $\hat{\mathcal{J}}_+$ of the temporary singularity; see **Figure 14**.

An example of such a diffeomorphism is given when $\mathcal{M}$ is Minkowski spacetime excluding the origin, and $\hat{\mathcal{M}}$ is Minkowski spacetime excluding the line $\hat{\mathcal{I}} = \{(\hat{t}, 0, 0, 0), -1 \leq \hat{t} \leq 1\}$. The interval $\hat{\mathcal{I}}$ would be timelike in Minkowski spacetime, and the diffeomorphism $\phi : \hat{\mathcal{M}} \to \mathcal{M}$ is given implicitly by

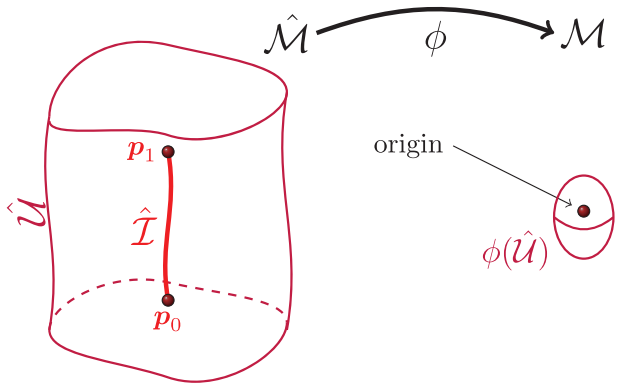

Figure 13. The diffeomorphism $\phi : \hat{\mathcal{M}} \to \mathcal{M}$ which maps a topological 3–sphere $\hat{\mathcal{U}}$ surrounding the temporary singularity to a topological 3–sphere $\phi(\hat{\mathcal{U}})$ surrounding the origin.

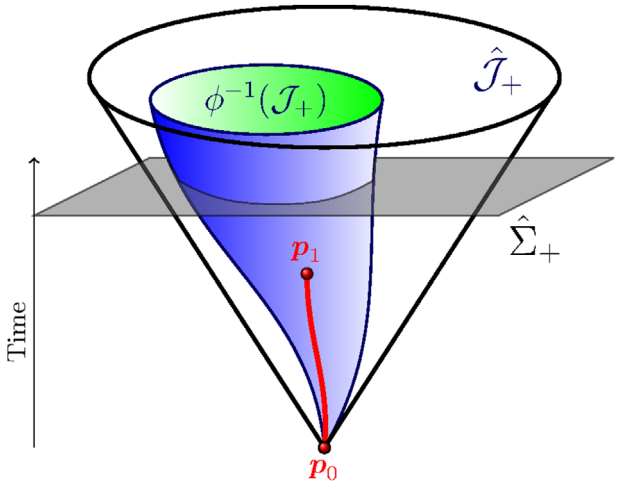

Figure 14. The domains in the morphed spacetime $\hat{\mathcal{M}}$. The distorted blue cone $\phi^{-1}(\mathcal{J}_+)$ is the causal cone pre-image of the causal cone cone $\mathcal{J}_+ \subset \mathcal{M}$. This lies inside the future causal cone $\hat{\mathcal{J}}_+$ of the temporary singularity, which is shown as an outlined white cone. The temporary singularity, which is not part of $\hat{\mathcal{M}}$, is indicated by the red curve between $\boldsymbol{p}_0$ and $\boldsymbol{p}_1$. Here, $\hat{\Sigma}_+$ is an arbitrary hypersurface intersecting $\hat{\mathcal{J}}_+$ away from the singularity.

$$\begin{aligned} \hat{t} &= t\left[1 + \left(t^2 + x^2 + y^2 + z^2\right)^{-1/2}\right], \\ \hat{x} &= x, \quad \hat{y} = y \quad \text{and} \quad \hat{z} = z \end{aligned} \tag{35}$$

as depicted in **Figure 15**. This diffeomorphism demonstrates that even though we cannot use a diffeomorphism to map a point into a line, we can nevertheless map the region around a point, into a region around a line.

An example with a spacelike temporary singularity by $\hat{\mathcal{M}} = \mathbb{R}^4 \backslash \hat{\mathcal{I}}$, $\hat{\mathcal{I}} = \{(0, \hat{x}, 0, 0), -1 \leq \hat{x} \leq 1\}$ is $\phi : \hat{\mathcal{M}} \to \mathcal{M}$ given implicitly by

$$\begin{aligned} \hat{t} &= t, \left[1 + \left(t^2 + x^2 + y^2 + z^2\right)^{-1/2}\right], \\ \hat{x} &= x, \quad \hat{y} = y \quad \text{and} \quad \hat{z} = z, \end{aligned} \tag{36}$$

as depicted in **Figure 16**.

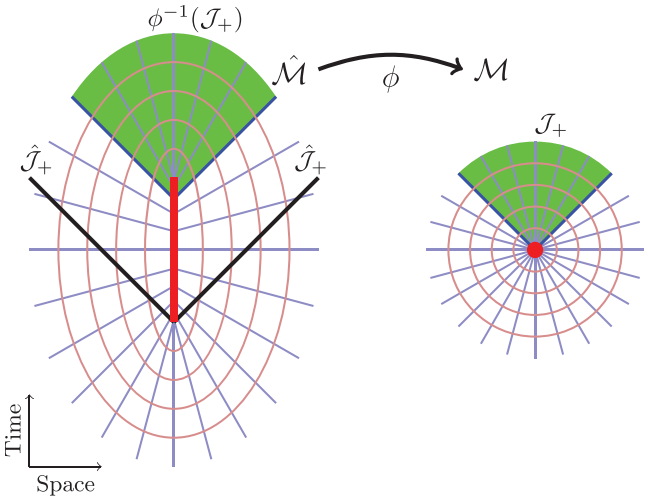

Figure 15. The diffeomorphism ϕ, given by Equation (35) which leads to a timelike singularity indicated by the red line. Here $\hat{\mathcal{J}}_+$ is bounded by the thick black lines whereas $\phi^{-1}(\mathcal{J}_+)$ is given by the green segment. The thick black lines are parallel to the boundary of the $\phi^{-1}(\mathcal{J}_+)$. The blue-gray lines in $\hat{\mathcal{M}}$ are mapped to radial lines in $\mathcal{M}$; likewise the light red ellipses are mapped to circles on $\mathcal{M}$. It is crucial to note that whilst ϕ maps $\hat{\mathcal{M}}$ to $\mathcal{M}$, the timelike line singularity is not contained within $\hat{\mathcal{M}}$, nor is the point singularity contained within $\mathcal{M}$, and so the mapping remains consistent with ϕ being a diffeomorphism.

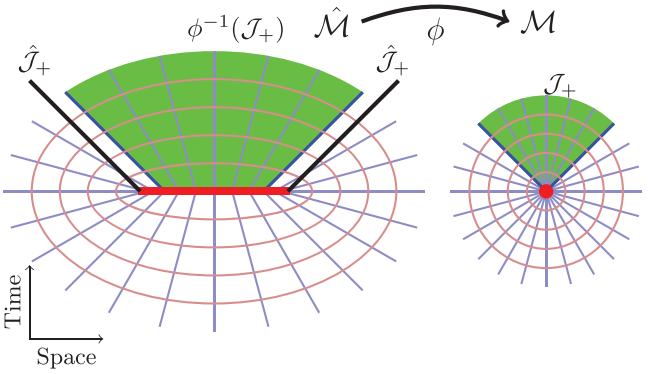

Figure 16. The diffeomorphism ϕ, given by Equation (36), which leads to a spacelike singularity, given by the red line. The conventions are as in Figure 15.

In the general case, with ϕ satisfying (α) and (β) above, let $\hat{\star}$ be the Hodge dual in $\hat{\mathcal{M}}$ corresponding to the metric $\hat{g}$, and let $\hat{F} \in \Gamma\Lambda^2\hat{\mathcal{M}}$, $\hat{\zeta} \in \Gamma\Lambda^1\hat{\mathcal{M}}$, $\hat{Z}_{\text{top}} \in \Gamma\Lambda^2\hat{\mathcal{M}}$ and $\hat{J} \in \Gamma\Lambda^3\hat{\mathcal{M}}$ be the corresponding fields/sources on $\hat{\mathcal{M}}$ given respectively by

$$\begin{aligned} &\hat{F} = \phi^\star F, \quad \hat{\zeta} = \phi^\star \zeta, \quad \hat{Z}_{\text{top}} = \phi^\star Z_{\text{top}} \\ &\text{and} \qquad \hat{J} = \phi^\star J + d\big(\hat{\star}\phi^\star F - \phi^\star \star F\big) \end{aligned} \tag{37}$$

where $\phi^* : \Gamma\Lambda^2\hat{\mathcal{M}} \to \Gamma\Lambda^2\hat{\mathcal{M}}$ is the pullback of ϕ, which, we note, commutes with the exterior derivative.[50] The latter two terms on the right hand side of the equation for $\hat{J}$ ensure that $\hat{F}$, $\hat{\zeta}$, and $\hat{J}$ satisfy an equation analogous to Equation (5). In fact, all the induced fields satisfy equations analogous to Equations (5), (12)–(14), and (18), that is

$$\begin{aligned} &d\hat{\star}\hat{F} + \hat{\zeta} \wedge \hat{F} = \hat{J}, \quad d\hat{F} = 0, \quad d\hat{J} = 0, \\ &d\hat{\zeta} = \hat{Z}_{\text{top}} \quad \text{and} \quad \hat{Z}_{\text{top}} \wedge \hat{F} = 0 \end{aligned} \tag{38}$$

Let $\hat{\Sigma}_+$ be a spacelike hypersurface which intersects $\hat{\mathcal{J}}_+$ and is away from the temporary singularity. Then, from Equation (17) and the fact that integrals are preserved under diffeomorphism, we have

$$\begin{aligned} \hat{Q}_+ &= \int_{\hat{\Sigma}_+} \hat{J} = \int_{\hat{\mathcal{U}}} \hat{J} = \int_{\hat{\mathcal{U}}} \left[\phi^\star J + d\big(\hat{\star}\phi^\star F - \phi^\star \star F\big)\right] \\ &= \int_{\hat{\mathcal{U}}} \phi^\star J + \int_{\partial\hat{\mathcal{U}}} \big(\hat{\star}\phi^\star F - \phi^\star \star F\big) = \int_{\hat{\mathcal{U}}} \phi^\star J \\ &= \int_{\mathcal{U}} J = Q_+ \neq 0 \end{aligned} \tag{39}$$

where $\hat{\mathcal{U}}$ is a topological 3–sphere which surrounds the singularity and $\mathcal{U} = \phi(\hat{\mathcal{U}})$.

Again we have satisfied (i)–(iii) and (a)–(e) and we conclude that the global charge is not conserved in the more general spacetime $\hat{\mathcal{M}}$.

7. Conclusion

In this article, we have investigated the behavior of charge conservation, a usually sacrosanct principle of standard electromagnetism. It has already been shown that it is possible to break global charge conservation whilst preserving local charge conservation,[11] and this was done by considering an extension of Maxwell's equations where the excitation fields $\boldsymbol{D}$ and $\boldsymbol{H}$ are no longer physical fields, and placing this in a spacetime containing a temporary singularity. This situation is in common with other consequences of singularities, where it is said that since "physics breaks down", anything might occur as a result. However, bearing in mind the H.G. Wells quote: "If anything is possible, then nothing is interesting", we were motivated to find examples that constrain this inchoate sense of the possibilities.

Here we have substantiated a situation where a minimally extended Maxwellian electromagnetism with an axionic coupling[12] in a topologically non-trivial spacetime fails to conserve global charge, by mathematically specifying the required space and time dependence of the relevant fields. In this construction there are no fields before the advent of the singularity, and the axions and charge emerge from it; the scheme can even be time reversed so as to destroy correctly configured and collapsing arrangements of axions and charge. Attempts to recover global charge conservation by accounting for the axionic charge "in" the singularity (before it emerges into the universe) are bound to fail as we have deliberately restricted attention to situations that are diffeomorphic to an instantaneous singularity. Further, our specification can be transformed by diffeomorphism to apply also to a range of related scenarios, including that for singularity that lives for a finite time. In doing this we have also demonstrated that although in a general sense anything might happen at a singularity, in practise *anything* will not. This

is because the spacetime surrounding the singularity is subject to physical law, which constrains the means by which the "anything" can happen.

It is, however, certainly arguable that the form of the solutions is somewhat contrived, that is, that no such field configuration will form randomly or be created naturally. However, in the spirit of Morris and Thorne's famous paper on wormholes[51] we can ask "What constraints do the laws of physics place on the activities of an arbitrarily advanced civilization?" Suppose an advanced civilization feels it is necessary to adjust the total charge of the universe, having predicted – or perhaps manufactured – the arrival of a temporary singularity. They will then be able to construct the fields F, ζ_{top}, and Z_{top} in such a way that they will all vanish, along with axionically driven charge ($Q_{-} = \int_{\Sigma_{-}} \zeta \wedge F$), into singularity.

Our conclusion appears to be at once startling and undeniable: global charge conservation cannot be guaranteed in the presence of axionic electromagnetic interaction.

Appendix A: Depicting Forms as Curves and Surfaces

It is extremely useful to represent forms pictorially by dots, curves, and surfaces,[49] because once the conventions are learnt, it enables information to be conveyed more easily and more accurately. In four dimensions a 1–form is given by 3D volumes, a 2–form by 2D surfaces, and a 3–form by 1D curves. Closed forms are submanifolds that do not have boundaries, while non-closed forms do have boundaries.

These submanifolds (forms) have an orientation, where untwisted forms have an external orientation while twisted forms have internal orientation. To show these submanifolds for our field solution, we have used two slices. Both slices are at $t = 10$, but with $\theta = 0$ in **Figure A1**, contrasting with an orthogonal slice at $z = 0$ in **Figure A2**. Figure A2 also shows the orientations of

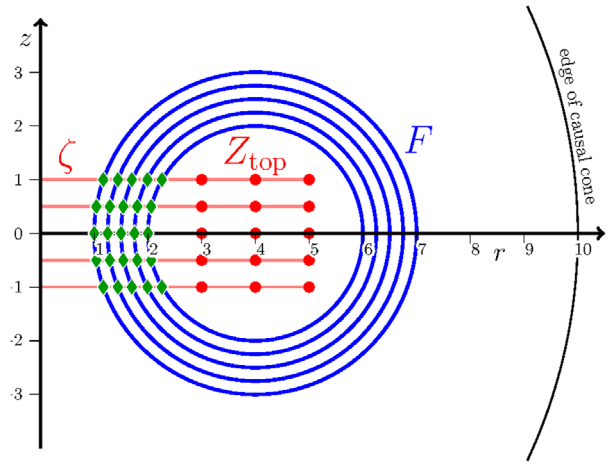

Figure A1. Representing the four fields on a slice at $\theta = 0$ at $t = 10$, showing the r, z plane. Here the timeslice submanifolds of F overlap the $\theta = 0$ plane, and so are shown as blue circles, as per Table A1. The two axionic fields – ζ (light red) and Z_{top} (dark red) – have timeslice submanifolds that intersect with the $\theta = 0$ plane, and so are depicted as lines and dots. Last, the points of the timeslice submanifold for $\zeta \wedge F$ are shown as green diamonds. This is the same view as on Figure 7.

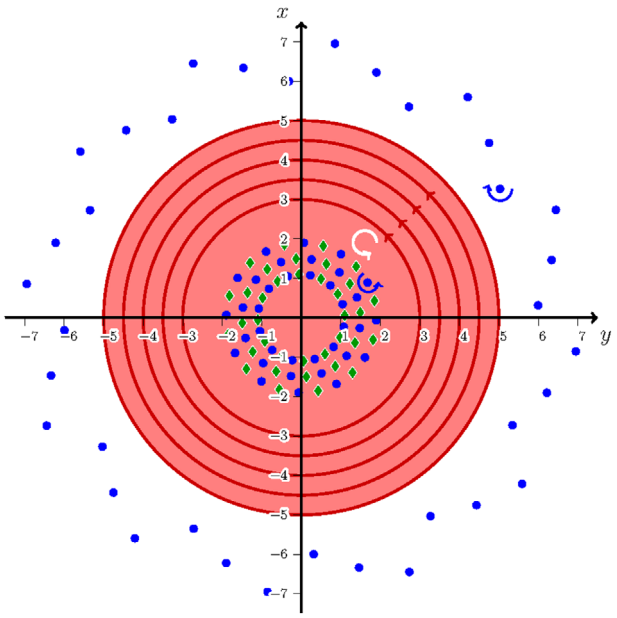

Figure A2. Representing the four fields on a slice $z = 0$ at $t = 10$, showing the x, y (or r, θ) plane. Here F has timeslice submanifolds that intersect with the $z = 0$ plane, and so are depicted as blue dots. The two axionic fields – ζ (light red) and Z_{top} (dark red) – have timeslice submanifolds that overlap the $z = 0$ plane, and so are shown as a disc and circles as per Table A1. Last, the points of the timeslice submanifold for $\zeta \wedge F$ are shown as green diamonds. The orientations of F in this diagram are indicated by blue arrows curling around selected dots, and the orientation of ζ by a white curled arrow. This is the same view as in Figure 12.

Table A1. The four fields F, ζ, Z_{top}, and $F \wedge \zeta$ and how they are depicted in Figures A1 and A2.

Form	Degree	Parity	Submanifold on timeslice	Color
F	2	untwisted	1D circles in (r, z) plane	blue
ζ	1	twisted	2D disc in (r, θ) plane	light red
Z_{top}	2	twisted	1D circles in (r, θ) plane	dark red
$F \wedge \zeta$	3	twisted	0D dots	green

the fields. In **Table A1**, we list the four fields F, ζ, Z_{top}, and $F \wedge \zeta$. We show how they are depicted in Figures A1 and A2.

For the timeslice $t = 10$, the electromagnetic 2–form F is a set of closed surfaces, and on the intersection with $\theta = 0$, are represented by circles, as can be seen on Figure A1. These circles lie in the (r, z) plane and on the intersection with $z = 0$, F is represented as dots, as depicted in Figure A2. Since F is an untwisted form, their orientation is external and in Figure A2 can be shown as an arrow which curls round the blue F dots. Since the blue F circles in Figure A1 come out of the $z = 0$ plane in the region $6 < r < 7$, and go into the plane in the region $1 < r < 2$, they have opposite orientations in these two regions. These blue circles also mimic the magnetic field lines. The electric field is then perpendicular to these circles, pointing toward the next circle of the same radius at greater θ.

The 2–form axion flux Z_{top}, depicted in dark red, is represented by circles in the $(r, \theta) = (x, y)$ plane. These are twisted, so have

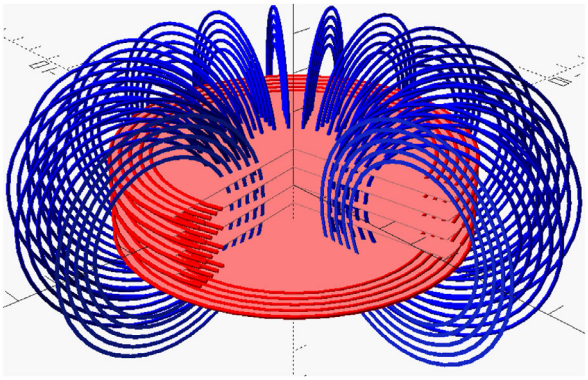

Figure A3. A 3D representation of the F (blue), ζ (light red), and Z_{top} (dark red) submanifolds on a timeslice. Each of the three field elements has a 90° wedge cut out, with each wedge rotationally offset by a small angle, to help show and clarify interior detail.

an internal orientation which is shown as anticlockwise in Figure A2.

The 1–form axion field ζ, depicted in light red, is represented by discs in the (r, θ) planes. These are twisted, so have an internal orientation which is shown as shown (in white) as anticlockwise in Figure A2. This is because it is compatible with the orientation of Z_{top}.

The 3–form $\zeta \wedge F$, depicted as green diamonds. These diamonds are in the region where the supports of ζ and F intersect. Since the orientation of ζ and F are the same in this region, the orientation of $\zeta \wedge F$ is simply "+". In spacetime this 3–form is depicted as lines, that is straight line flowing outward from the origin. The internal orientations are arrows pointing out of the page.

A 3D view of the field forms is shown in **Figure A3**. Indeed, this visualization is particularly useful when considering how such a field configuration could be generated. We see that in the snapshot, the $\boldsymbol{B}$ field lines need to form a cylinder of field loops bent around into a torus. Such an arrangement might be achieved using electric currents passing in opposite directions along a pair of hollow concentric wires, with the magnetic field thus localized between them. Conveniently, the electric field $\boldsymbol{E}$ can then arise naturally, because the solution – and hence the tori – are expanding with time, and that time-dependent $\boldsymbol{B}$ field directly produces $\boldsymbol{E}$. Further, we can see that the axion flux Z_{top} is oriented along loops around the main axis, representing a circulating flux consistent with the axion field ζ.

Appendix B: Proof About the Future Causal Cone $\mathcal{J}_+$

Proof of Equation (11). Observe that if $p \in \mathcal{J}_+^{\text{sup}}(\mathcal{I})$ then there is a causal curve connecting $\mathcal{I}$ to p. This will intersect every 3–sphere $\mathcal{U}$ between $\mathcal{I}$ to p. By contrast if $p \notin \mathcal{J}_+^{\text{sup}}(\mathcal{I})$ then there exists a 3–sphere surrounding $\mathcal{I}$ which does not intersect the backward causal cone of p.

Appendix C: Remarks on a Lagrangian

Another interesting question is whether or not it is easy to construct a Lagrangian for our topological axion field: the presence of a Lagrangian would assure us that our model has features convenient for a wider context, such as the derivation of the corresponding stress-energy tensor, consequent conservation laws, and even path-integrals. A Lagrangian can be constructed if we also assume that $A \wedge Z_{\text{top}} = 0$, where A is the electromagnetic potential.[52] With this Lagrangian as the integrand, Equation (5) follows by varying the action

$$S[A] = \int \left(\tfrac{1}{2} dA \wedge \star dA - A \wedge J + \tfrac{1}{2} A \wedge \zeta \wedge dA \right) \tag{C1}$$

with respect to A, where $F = dA$.

To motivate this Lagrangian, note that when varying S with respect to A we have

$$\begin{aligned}
\delta S &= \int \Big(\tfrac{1}{2} d\delta A \wedge \star dA + \tfrac{1}{2} dA \wedge \star d\delta A \\
&\qquad - \delta A \wedge J + \tfrac{1}{2} \delta A \wedge \zeta \wedge dA + \tfrac{1}{2} A \wedge \zeta \wedge d\delta A \Big) \\
&= \int \left(d\delta A \wedge \star dA - \delta A \wedge J + \tfrac{1}{2} \delta A \wedge \zeta \wedge dA - \tfrac{1}{2} d(A \wedge \zeta) \wedge \delta A \right) \\
&= \int \Big(\delta A \wedge d \star dA - \delta A \wedge J + \tfrac{1}{2} \delta A \wedge \zeta \wedge dA - \tfrac{1}{2} dA \wedge \zeta \wedge \delta A \\
&\qquad - \tfrac{1}{2} A \wedge d\zeta \wedge \delta A \Big) \\
&= \int \delta A \wedge \left(d \star dF - J + \zeta \wedge dA + \tfrac{1}{2} A \wedge Z_{\text{top}} \right).
\end{aligned} \tag{C2}$$

However, as stated, although we require that $A \wedge Z_{\text{top}} = 0$, it is important to note that, since A is a potential, it is not globally defined. Thus we can only assume we can find a topologically trivial region of $\mathcal{M}$ where A is defined such that $A \wedge Z_{\text{top}} = 0$. In this case Equation (5), our axionic Maxwell–Ampère–Gauss equation does follow from Equation (C1). Although we do not claim that it is always possible to find such a region, in the solution presented here $F \wedge Z_{\text{top}} = 0$, and we can therefore locally choose gauges where $A \wedge Z_{\text{top}} = 0$.

Appendix D: Spacetime Metric and the Proof of Equation (20)

Proof. Since

$$\begin{aligned}
&Z_{\text{SE}} \wedge \widetilde{V} \wedge \star \left(B \wedge \widetilde{V} \right) \\
&= Z_{\text{SE}} \wedge \widetilde{V} \wedge i_V \star B = i_V (Z_{\text{SE}} \wedge \widetilde{V}) \wedge \star B \\
&= -Z_{\text{SE}} \wedge (i_V \widetilde{V}) \wedge \star B = Z_{\text{SE}} \wedge \star B = g(Z_{\text{SE}}, B) \star 1
\end{aligned} \tag{D1}$$

Likewise

$$\star \left(dt \wedge Z_{\text{SB}} \right) \wedge (dt \wedge E) = (dt \wedge E) \wedge \star \left(dt \wedge Z_{\text{SB}} \right) = g(Z_{\text{SB}}, E) \star 1 \tag{D2}$$

Also from the star pivot

$$\begin{aligned}
\star \left(dt \wedge Z_{\text{SB}} \right) \wedge \star \left(dt \wedge Z_{\text{SB}} \right) &= \left(dt \wedge Z_{\text{SB}} \right) \wedge \star \star \left(dt \wedge Z_{\text{SB}} \right) \\
&= -\left(dt \wedge Z_{\text{SB}} \right) \wedge \left(dt \wedge Z_{\text{SB}} \right) = 0
\end{aligned} \tag{D3}$$

From Equation (18) we have

$$\begin{aligned} 0 = Z_{\text{top}} \wedge F &= \left(dt \wedge Z_{\text{SE}} + \star\left(dt \wedge Z_{\text{SB}}\right)\right) \wedge (dt \wedge E + \star\,(dt \wedge B)) \\ &= dt \wedge Z_{\text{SE}} \wedge \star(dt \wedge B) + \star\left(dt \wedge Z_{\text{SB}}\right) \wedge (dt \wedge E) \\ &+ \star\left(dt \wedge Z_{\text{SB}}\right) \wedge \star\left(dt \wedge Z_{\text{SB}}\right) \\ &= (g(Z_{\text{SB}}, E) + g(Z_{\text{SE}}, B)) \star 1 \end{aligned} \tag{D4}$$

□

Acknowledgements

Both J.G. and P.K. are grateful for the support provided by STFC (Cockcroft Institute, ST/G008248/1 and ST/P002056/1) and EPSRC (Alpha-X, EP/N028694/1). P.K. would also like to acknowledge recent support from the UK National Quantum Hub for Imaging (QUANTIC, EP/T00097X/1).

Conflict of Interest

The authors declare no conflict of interest.

Data Availability Statement

Further information (and any data) are available from the corresponding author upon reasonable request.

Keywords

charge conservation, constitutive relations, electromagnetism, gauge freedom, topology

Received: November 20, 2020
Revised: February 26, 2021
Published online: May 5, 2021

[1] E. Curiel, *Philos. Sci.* **1999**, *66*, S119.
[2] E. Curiel, Singularities and Black Holes, *The Stanford Encyclopedia of Philosophy* (Spring 2021 Edition), Edward N. Zalta (ed.), https://plato.stanford.edu/archives/spr2021/entries/spacetime-singularities/
[3] J. Earman, *Foundations of Physics* **1996**, *26*, 623.
[4] M. A. Scheel, K. S. Thorne, *Phys.-Usp.* **2014**, *57*, 342.
[5] A. D. Alawneh, R. P. Kanwal, *SIAM Rev.* **1977**, *19*, 437.
[6] N. R. Heckenberg, R. McDuff, C. P. Smith, A. G. White, *Opt. Lett.* **1992**, *17*, 221.
[7] S. A. R. Horsley, I. R. Hooper, R. C. Mitchell-Thomas, O. Quevedo-Teruel, *Sci. Rep.* **2014**, *4*, 4876.
[8] S. Coleman, S. Hughes, *Phys. Lett. A* **1993**, *309*, 246.
[9] J. Earman, in *Bangs, Crunches, Whimpers, and Shrieks: Singularities and Acausalities in Relativistic Spacetimes*, Oxford University Press, Oxford **1995**, Ch. 3.
[10] If spacetime $\mathcal{M}$ has a non-zero third de Rham cohomology $H^3_{\text{dR}(\mathcal{M})} \neq 0$, then there exists a closed 3–form current J which is not exact, that is $dJ = 0$ but $J \neq d\mathcal{H}$ for any excitation 2–form field $\mathcal{H}$. Hence for 3–surfaces $\mathcal{V}$ enclosing the temporary singularity $\int_{\mathcal{V}} J \neq 0$.
[11] J. Gratus, P. Kinsler, M. W. McCall, *Found. Phys.* **2019**, *49*, 330.
[12] J. Gratus, M. W. McCall, P. Kinsler, *Phys. Rev. A* **2020**, *101*, 043804.
[13] D. Lai, W. G. C. Ho, *Astrophys. J.* **2003**, *588*, 962.
[14] W. Heisenberg, H. Euler, *Z. Physik* **1936**, *98*, 714.
[15] F. Bopp, *Ann. Phys. (Berlin)* **1940**, *430*, 345.
[16] B. Podolsky, *Phys. Rev.* **1942**, *62*, 68.
[17] J. Gratus, V. Perlick, R. W. Tucker, *J. Phys. A* **2015**, *48*, 435401.
[18] J. D. Jackson, *Classical Electrodynamics*, 3rd ed., Wiley, Hooboken, Germany **1999**.
[19] J. Gratus, P. Kinsler, M. W. McCall, *Eur. J. Phys.* **2019**, *40*, 025203.
[20] J. A. Heras, *Am. J. Phys.* **2011**, *79*, 409.
[21] J. J. Roche, *Am. J. Phys.* **2000**, *68*, 438.
[22] J. Roche, *Eur. J. Phys.* **1998**, *19*, 155.
[23] M. Landini, *Prog. Electromagn. Res.* **2014**, *144*, 329.
[24] A. M. Bork, *Am. J. Phys.* **1963**, *31*, 854.
[25] S. M. Carroll, G. B. Field, R. Jackiw, *Phys. Rev. D* **1990**, *41*, 1231.
[26] D. Colladay, V. A. Kostelecky, *Phys. Rev. D* **1998**, *58*, 116002.
[27] Y. Itin, *Phys. Rev. D* **2004**, *70*, 025012.
[28] M. E. Tobar, B. T. McAllister, M. Goryachev, *Phys. Dark Universe* **2019**, *26*, 100339.
[29] L. Visinelli, *Mod. Phys. Lett. A* **2013**, *28*, 1350162.
[30] Y. N. Obukhov, F. W. Hehl, *Phys. Lett. A* **2005**, *341*, 357.
[31] I. Lindell, A. Sihvola, *IEEE Trans. Antennas Propag.* **2013**, *61*, 768.
[32] F. W. Hehl, Y. N. Obukhov, J.-P. Rivera, H. Schmid, *Phys. Lett. A* **2008**, *372*, 1141.
[33] R. Li, J. Wang, X.-L. Qi, S.-C. Zhang, *Nat. Phys.* **2010**, *6*, 284.
[34] L. Wu, M. Salehi, N. Koirala, J. Moon, S. Oh, *Science* **2016**, *354*, 1124.
[35] E. J. Post, *Formal Structure of Electromagnetics: General Covariance and Electromagnetics*, Dover Publications, Mineola, N.Y. **1997**.
[36] A. Lakhtakia, T. G. Mackay, *Proc. SPIE* **2015**, *9558*, 95580C.
[37] J. L. Feng, *Annu. Rev. Astron. Astrophys.* **2010**, *48*, 495.
[38] L. S. Dolin, *Izv. Vyssh. Uchebn. Zaved. Radiofizika* **1961**, *4*, 964.
[39] J. B. Pendry, D. Schurig, D. R. Smith, *Science* **2006**, *312*, 1780.
[40] M. McCall, J. B. Pendry, V. Galdi, Y. Lai, S. A. R. Horsley, J. Li, J. Zhu, R. C. Mitchell-Thomas, O. Quevedo-Teruel, P. Tassin, V. Ginis, E. Martini, G. Minatti, S. Maci, M. Ebrahimpouri, Y. Hao, P. Kinsler, J. Gratus, J. M. Lukens, A. M. Weiner, U. Leonhardt, I. I. Smolyaninov, V. N. Smolyaninova, R. T. Thompson, M. Wegener, M. Kadic, S. A. Cummer, *J. Opt.* **2018**, *20*, 063001.
[41] M. W. McCall, A. Favaro, P. Kinsler, A. Boardman, *J. Opt.* **2011**, *13*, 024003.
[42] P. Kinsler, M. W. McCall, *Photon. Nanostruct. Fundam. Appl.* **2015**, *15*, 10.
[43] J. Gratus, P. Kinsler, M. W. McCall, R. T. Thompson, *New J. Phys.* **2016**, *18*, 123010.
[44] S. Abdolrahimi, D. N. Page, C. Tzounis, *Phys. Rev. D* **2019**, *100*, 124038.
[45] Here $\Gamma\Lambda^p\mathcal{M}$ is the set of sections of the bundle $\Lambda^p\mathcal{M}$ of p–forms. That is the statement $F \in \Gamma\Lambda^2\mathcal{M}$ means F is a 2–form field on $\mathcal{M}$. However we usually just say F is a 2–form, with the fact it is a field being implicit.
[46] In terms of coordinates, the general $\Psi\langle F\rangle$ can be written using $i^a = g^{ab} i_{\partial_b}$, as $\Psi\langle F\rangle = (\frac{1}{2}\Psi^{abc} F_{bc} + \frac{1}{2}\Psi^{abcd}(\partial_b F_{cd})) \star dx_a$, where $\Psi^{abc} = i^a \star (\Psi\langle dx^b \wedge dx^c\rangle)$, and $\Psi^{abcd} = i^a \star (\Psi\langle x^b\, dx^c \wedge dx^d\rangle - x^b\, \Psi\langle dx^c \wedge dx^d\rangle)$.
[47] C. W. Misner, K. S. Thorne, J. A. Wheeler, *Gravitation*, W. H. Freeman, San Francisco **1973**.
[48] Note that there is no axion property (i.e. neither ζ nor Z_{top}) that contributes directly to the current in Maxwell equations; these axions carry no electric charge. There is therefore a clear distinction between the nature of the conventional current J and the axionic interaction term $\zeta \wedge F$. Nevertheless, it is interesting to note that if one were to claim $\zeta \wedge F$ as part of some new augmented current $J_{\text{new}} = J - \zeta \wedge F$, this J_{new} would be automatically conserved both globally and locally, since $d \star F = J_{\text{new}}$.
[49] J. Gratus, *arxiv1709.08492*, **2017**.
[50] J. Baez, J. P. Muniain, *Gauge fields, Knots and Gravity*, World Scien tific, Singapore **1994**.
[51] M. S. Morris, K. S. Thorne, *Am. J. Phys.* **1988**, *56*, 395.
[52] The constraint $A \wedge Z_{\text{top}} = 0$ is, however, harder to derive from an action.